Supporting Information

Wohlers et al. 10.1073/pnas.0812743106

SI Text

Autotrophic Growth, Community Composition, and Buildup of Organic Matter. With the onset of algal growth, an increase in primary production rates as measured by ^{14}C incorporation was observed (Fig. S2). The developing bloom was dominated by chain-forming diatoms (mainly *Skeletonema costatum*, *Chaetoceros minimum*, *Chaetoceros curvisetus*, and *Thalassiosira nordenskioldii*), contributing >95% to total phytoplankton abundance at the time of maximum biomass accumulation. The predominance of these species was also reflected in size-fractionated primary production measurements, showing that the vast majority of total primary production (Fig. S2*A*) occurred in the size fraction >3 μm (Fig. S2*B*). A significant response of primary production to temperature as depicted, for instance, by maximum rates of total primary production was not observed ($P = 0.76$).

Moreover, the stoichiometric composition of the accumulating particulate organic matter, i.e., the ratio of particulate organic carbon to nitrogen (C/N) and phosphorus (C/P), was not notably affected by rising temperature. At the time of maximum biomass accumulation the C/N and C/P ratios deviated from the Redfield ratio with average values of 15.0 ± 2.2 and 544.3 ± 69.1, but were not significantly correlated to temperature ($P_{C/N} = 0.42$; $P_{C/P} = 0.78$).

Possible Causes of Organic Carbon Loss (ΔC_{loss}) from the Water Column. In principle, 3 processes may account for the loss of carbon from the water column: (*i*) CO_2 outgassing, (*ii*) organic carbon fixation through algal growth on mesocosm walls, and (*iii*) sinking of organic matter to the bottom of the mesocosms. As photosynthetic carbon uptake caused a decline in mesocosm pCO_2 below the atmospheric level of 380 ppm, resulting in a net flux of CO_2 into the mesocosm water, outgassing can be excluded as a loss term. Moreover, DIC concentrations were corrected for the air-water exchange of CO_2 (see *Materials and Methods* for details on calculations). Based on repeated inspections of the mesocosm walls, carbon loss through fouling was also found to be negligible. In contrast, accumulation of particulate matter at the bottom of the enclosures was prominent in all treatments. Although attempts to obtain quantitative measurements of the amount of particulate matter accumulating at the bottom of the enclosures were impeded by its highly patchy distribution, a crude extrapolation of POC measured in individual patches confirmed that bottom accumulation represented the predominant loss term for carbon from the water column. A similar temperature effect on the sinking of particulate matter was also observed in other mesocosm studies, where the amount of organic carbon lost via sedimentation decreased with increasing temperature (1, 2).

Temperature Sensitivity of Aggregation Processes. With the onset of the phytoplankton bloom, the concentration of TEP began to increase in all treatments (Fig. S4*A*). A second and much more pronounced increase in TEP concentration occurred in the postbloom phase of the T+6 and to a lesser extent in the T+4 treatments, but was absent in the T+2 and T+0 treatments. Concurrent to the increase in TEP at elevated temperatures, we observed a decrease in polysaccharide concentration (PCHO) (Fig. S4*B*), indicating that TEP was formed by aggregation of the polysaccharide fraction of DOC. Lower concentrations of PCHO in the T+2 and T+0 treatments may have limited TEP formation, which may explain the observed decrease in TEP concentrations during bloom decline.

Transformation of dissolved into particulate organic matter via abiotic aggregation to TEP was shown both in laboratory (3, 4) and mesocosm studies (5). Because of their surface-reactive nature, TEP promote the aggregation and sinking of particulate matter (6, 7). To what extent enhanced TEP formation affected particle sinking in our study is, however, difficult to assess. TEP concentrations in the elevated temperature treatments showed the strongest increase at a time when particulate matter concentrations had nearly decreased to prebloom levels, hence limiting the potential for TEP-mediated particle export.

Materials and Methods. Samples for dissolved carbohydrates were filtered through precombusted (5 h, 450 °C) GF/Fs. The filtrate was collected in precombusted (12 h, 450 °C) glass vials and stored at −20°C. The analysis was carried out using the 2,4,6-tripyridyl-s-triazine (TPTZ) spectrophotometric method (8).

The concentration of TEP was determined colorimetrically (9). Samples were gently (<150 mbar) filtered through 0.4-μm polycarbonate filters (Whatman), stained with Alcian Blue and stored at −20°C until analysis. The dye was redissolved in 80% H_2SO_4 for 3 h and the supernatant analyzed on a Hitachi U-2000 spectrophotometer. All filters were prepared in duplicate. The acidic polysaccharide Gum Xanthan was used as a standard. The carbon content of TEP (μmol $C{\cdot}L^{-1}$) was calculated by using a conversion factor ($f' = 0.63$) (6).

Primary production (PP) was determined through measurements of ^{14}C-bicarbonate ($H^{14}CO_3^-$) uptake (10, 11). For this purpose, $H^{14}CO_3^-$ was added to 30-ml samples at a final activity of 4 μCi per bottle. The samples were then incubated in situ for 4–5 h at intermediate water depth inside the respective mesocosms. All incubations were carried out in duplicate with 1 dark bottle serving as a blank. After incubation, sample aliquots were filtered onto 0.2-μm cellulose acetate and 3.0-μm polycarbonate filters, respectively. The filters were fumed with concentrated hydrochloric acid (HCl) for 10 min to remove excess $H^{14}CO_3^-$. Finally, samples were radio-assayed in 4 ml of scintillation mixture (Lumagel Plus) on a Packard TriCarb scintillation counter. Daily PP (μmol $C{\cdot}L^{-1}{\cdot}d^{-1}$) was calculated by multiplying the obtained production rates with a light factor (total amount of light throughout the day divided by the amount of light received during the incubation).

1. Keller AA, Oviatt CA, Walker HA, Hawk JD (1999) Predicted impacts of elevated temperature on the magnitude of the winter-spring phytoplankton bloom in temperate coastal waters: A mesocosm study. *Limnol Oceanogr* 44:344–356.
2. Müren U, Berglund J, Samuelsson K, Andersson A (2005) Potential effects of elevated sea-water temperature on pelagic food webs. *Hydrobiologia* 545:153–166.
3. Chin W-C, Orellana MV, Verdugo P (1998) Spontaneous assembly of marine dissolved organic matter into polymer gels. *Nature* 391:568–572.
4. Kerner M, Hohenberg H, Ertl S, Reckermann M, Spitzy A (2003) Self-organization of dissolved organic matter to micelle-like microparticles in river water. *Nature* 422:150–154.
5. Engel A, Thoms S, Riebesell U, Rochelle-Newall E, Zondervan I (2004) Polysaccharide aggregation as a potential sink of marine dissolved organic carbon. *Nature* 428:929–932.
6. Engel A (2004) Distribution of transparent exopolymer particles (TEP) in the northeast Atlantic Ocean and their potential significance for aggregation processes. *Deep-Sea Res I* 51:83–92.
7. Passow U, Alldredge AL (1994) Aggregation of a diatom bloom in a mesocosm: The role of transparent exopolymer particles (TEP). *Deep-Sea Res II* 42:99–109.
8. Myklestad S, Skånøy E, Hestmann S (1997) A sensitive and rapid method for analysis of dissolved mono- and polysaccharides in seawater. *Mar Chem* 56:279–286.

9. Passow U, Alldredge AL (1995) A dye-binding assay for the spectrophotometric measurement of transparent exopolymer particles (TEP). *Limnol Oceanogr* 40:1326–1335.
10. Gargas E (1975) A manual for phytoplankton primary production studies in the Baltic. *Baltic Mar Biol* 2:1–88.
11. Steemann Nielsen E (1952) The use of radioactive carbon (^{14}C) for measuring production in the sea. *J Cons Int Explor Mer* 18:117–140.

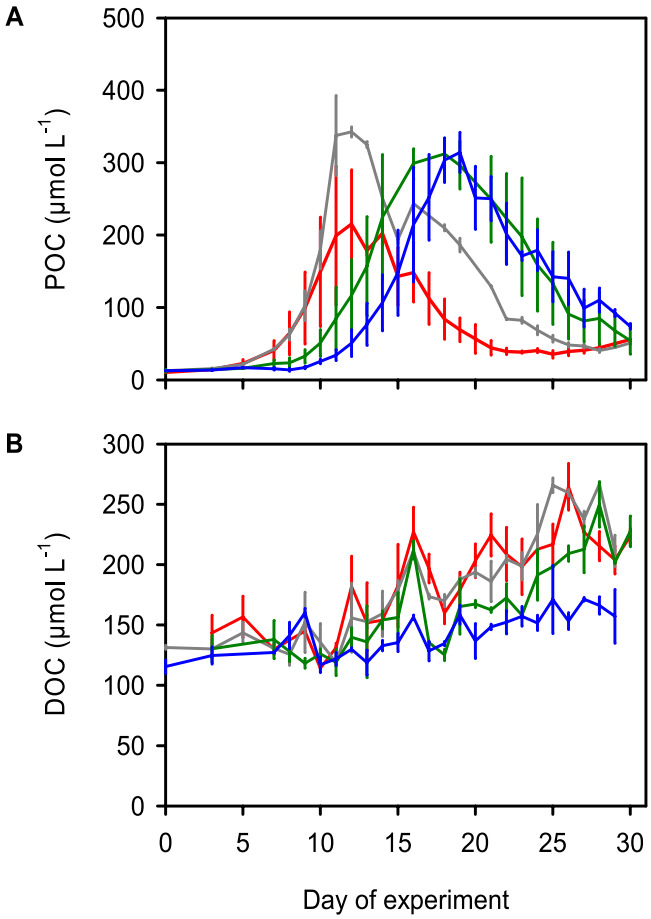

Fig. S1. Temporal development of POC (*A*) and DOC (*B*) concentrations. The different colors represent the 4 temperature regimes: the in situ temperature T+0 (blue) and the elevated temperature regimes T+2 (green), T+4 (gray), and T+6 (red). Solid lines denote the average of 2 replicate mesocosms; error bars indicate the range of the replicates.

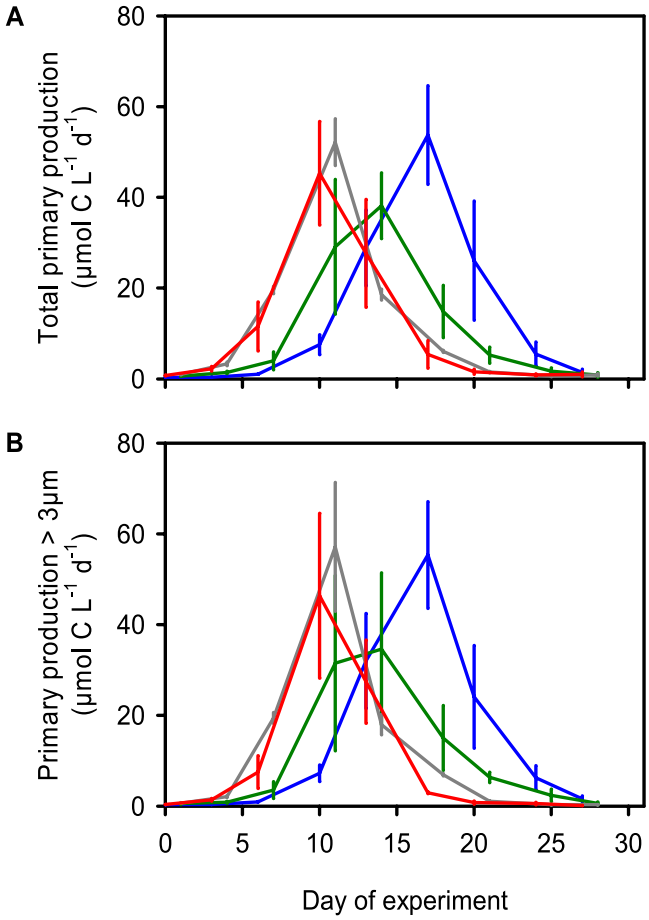

Fig. S2. Temporal development of autotrophic primary production. Rates of total primary production (>0.2 μm) (*A*) and primary production in the size fraction >3 μm (*B*). Color and symbol codes are as in Fig. S1.

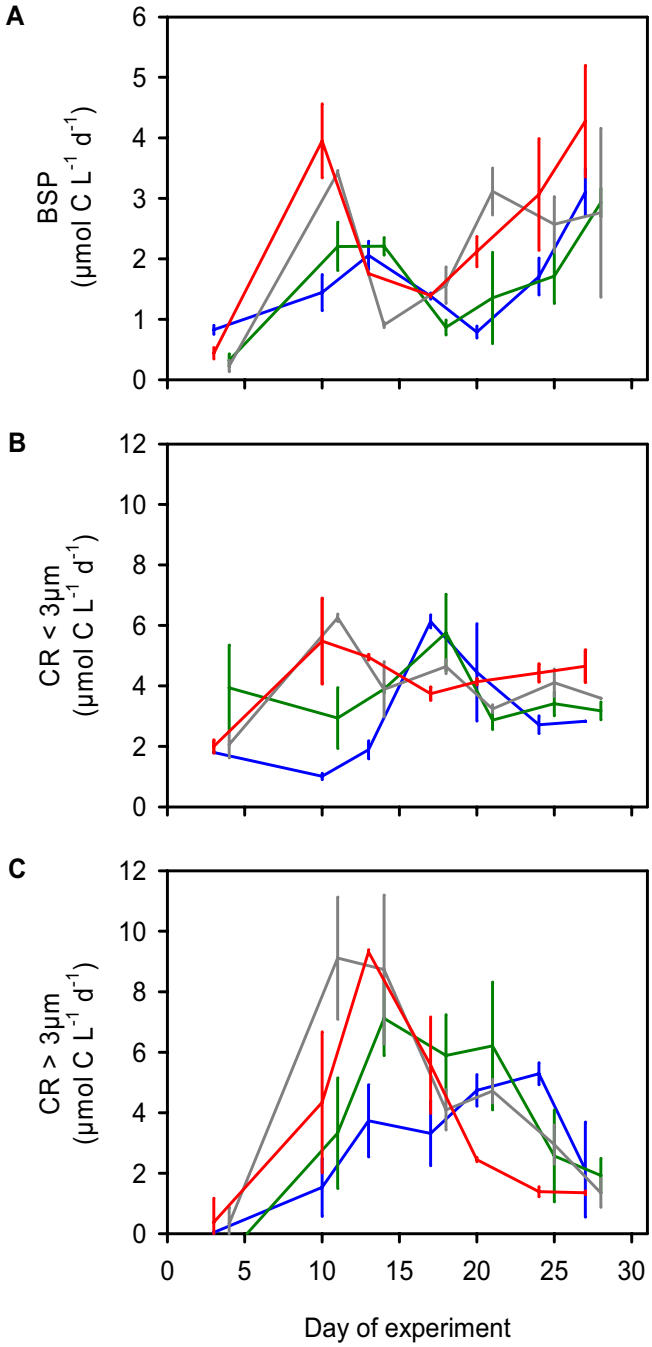

Fig. S3. Temporal development of bacterial secondary production and community respiration. (*A*) BSP rates of free-living bacteria (<3 μm) as calculated from ^{3}H-leucine uptake. (*B* and *C*) CR rates in the bacterial size fraction (CR <3 μm) and the nonbacterial size fraction (CR >3 μm). Color and symbol codes are as in Fig. S1.

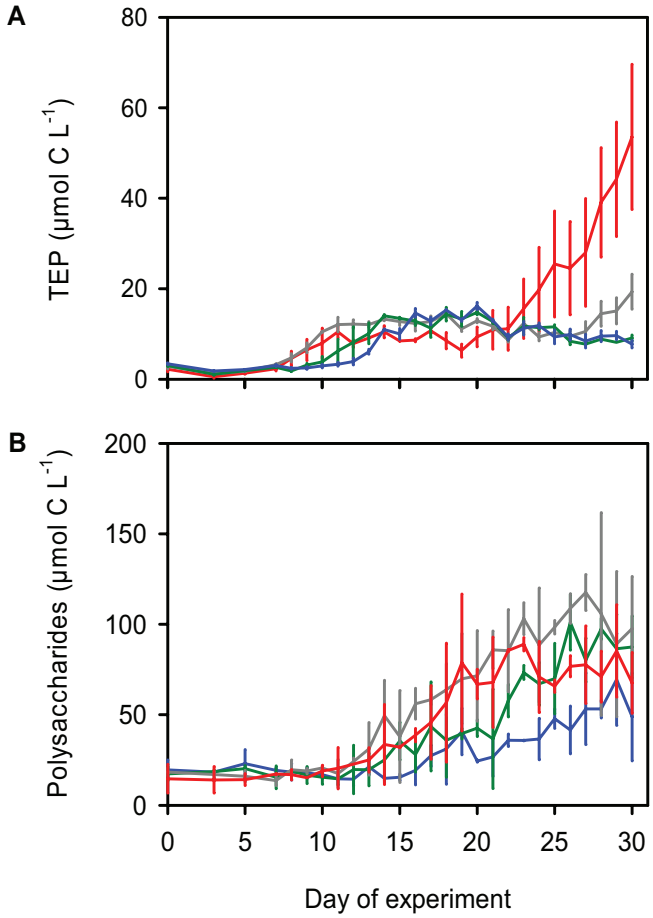

Fig. S4. Temporal development of transparent exopolymer particles and dissolved polysaccharides. (*A*) TEP. (*B*) PCHO. Color and symbol codes are as in Fig. S1.

Table S1. Water temperature and light intensity

Statistic	Mesocosm no.							
	T+0_1	T+0_2	T+2_1	T+2_2	T+4_1	T+4_2	T+6_1	T+6_2
Mean water temperature	2.1	2.4	4.1	4.8	5.9	6.5	7.0	8.0
Maximum light intensity, μmol photons$\cdot$ $m^{-2}\cdot s^{-1}$	177	201	193	204	187	171	127	176

Light/dark cycle was 12:12 h. Initial nutrient concentration (μmol$\cdot L^{-1}$) was 21.1 $\pm$ 0.20 for NO_3^-, 5.6 $\pm$ 0.30 for NH_4^+, 0.9 $\pm$ 0.01 for PO_4^{3-}, and 20.4 $\pm$ 0.50 for $Si(OH)_4$.